Available online at www.sciencedirect.com
ScienceDirect
Nanomedicine: Nanotechnology, Biology, and Medicine 5 (2009) 410–418
nanomedicine
www.nanomedjournal.com

Research Article

PEGylated PLGA nanoparticles for the improved delivery of doxorubicin

Jason Park, MS[a], Peter M. Fong, PhD[a], Jing Lu, PhD[b], Kerry S. Russell, MD, PhD[c], Carmen J. Booth, DVM, PhD[d], W. Mark Saltzman, PhD[a,*], Tarek M. Fahmy, PhD[a]

[a]*Department of Biomedical Engineering, Yale University, New Haven, Connecticut, USA*
[b]*Carigent Therapeutics, Inc., New Haven, Connecticut, USA*
[c]*Department of Internal Medicine, Cardiology, Yale Cardiology, The Anylan Center, New Haven, Connecticut, USA*
[d]*Section of Comparative Medicine, Yale Medical School, New Haven, Connecticut, USA*

Received 5 November 2008; accepted 13 February 2009

Abstract

We hypothesize that the efficacy of doxorubicin (DOX) can be maximized and dose-limiting cardiotoxicity minimized by controlled release from PEGylated nanoparticles. To test this hypothesis, a unique surface modification technique was used to create PEGylated poly(lactic-co-glycolic acid) (PLGA) nanoparticles encapsulating DOX. An avidin-biotin coupling system was used to control poly(ethylene glycol) conjugation to the surface of PLGA nanoparticles, of diameter ~130 nm, loaded with DOX to 5% (wt/wt). Encapsulation in nanoparticles did not compromise the efficacy of DOX; drug-loaded nanoparticles were found to be at least as potent as free DOX against A20 murine B-cell lymphoma cells in culture and of comparable efficacy against subcutaneously implanted tumors. Cardiotoxicity in mice as measured by echocardiography, serum creatine phosphokinase (CPK), and histopathology was reduced for DOX-loaded nanoparticles as compared with free DOX. Administration of 18 mg/kg of free DOX induced a sevenfold increase in CPK levels and significant decreases in left ventricular fractional shortening over control animals, whereas nanoparticle-encapsulated DOX produced none of these pathological changes.

From the Clinical Editor: The efficacy of doxorubicin (DOX) may be maximized and dose-limiting cardiotoxicity minimized by controlled release from PEGylated nanoparticles. Administration of 18 mg/kg of free DOX induced a sevenfold increase in CPK levels and significant decreases in left ventricular fractional shortening in mice, whereas nanoparticle-encapsulated DOX produced none of these pathological changes.

Key words: Doxorubicin; PLGA; PEGylated; Nanoparticle; Drug delivery

The encapsulation of cytotoxic chemotherapeutic agents in biodegradable poly(lactic-co-glycolic acid) (PLGA) nanoparticles may offer advantages over other delivery systems, including liposomes. A few of those advantages are well known and have been demonstrated in previous studies: a wide variety of agents—from extremely hydrophobic to highly hydrophilic[1]—can be encapsulated in PLGA nanoparticles, drug release rates can be tailored to particular applications,[2] and size and loading are easily manipulated to provide further control over drug delivery.[3] However, it has proven surprisingly difficult to produce surface-modified, drug-loaded PLGA particles. For example, the addition of poly(ethylene glycol) (PEG) to nanoparticle surfaces (i.e., PEGylation) is known to enhance circulation time by inhibition of nonspecific protein adsorption, opsonization, and subsequent clearance. This has been well demonstrated with PEGylated liposomes,[4] but a wide variety of attempts to similarly modify PLGA nanoparticles have yet to yield comparable results.[5] The difficulty in production of PEGylated PLGA particles has been speculated to be the result of insufficient or nonrobust surface attachment of PEG.[5] Effective PEGylation of particles implies a high-density coating with PEG, which has been difficult to achieve.

The difficulty associated with surface-modifying PLGA particles has been the lack of functional chemical groups on the aliphatic polyester backbone of the polymer. A variety of techniques have been developed for PEGylation of PLGA nanoparticles, such as adsorption,[6] incorporation of polymer conjugates (e.g., PLA-PEG),[7] or covalent attachment via amino or carboxyl-terminated PLGA,[8] but these methods

This work was supported by a grant to W.M.S. from the National Institutes of Health (EB000487) and a career award to T.M.F. from the Wallace Coulter Foundation.

*Corresponding author.
E-mail address: mark.saltzman@yale.edu (W.M. Saltzman).

1549-9634/$ – see front matter © 2009 Elsevier Inc. All rights reserved.
doi:10.1016/j.nano.2009.02.002

suffer from drawbacks such as low density or decreased presentation over time. Recently we developed a method for surface modification of drug-loaded PLGA particles that yields a robust and high-density attachment of ligands to the particle surface. In this report we used this new method to fabricate PEGylated PLGA particles and examined their clinical utility for the safe and effective delivery of the anticancer agent doxorubicin (DOX).

DOX is a highly potent antineoplastic agent approved for use against a wide spectrum of tumors. Unfortunately, its long-term clinical use is compromised by toxicities common to anthracycline drugs, the most serious being irreversible cardiomyopathy and subsequent congestive heart failure.[9] One proven strategy for limiting DOX cardiac toxicity has been to encapsulate the drug in carriers that decrease dose delivery to the heart and increase dose delivery to tissues harboring tumors. For example, encapsulation of DOX in PEGylated liposomes (such as the commercial preparation DOXIL; Bedford Laboratories, Bedford, Ohio) results in decreased DOX-induced cardiomyopathy while preserving antitumor activity against certain solid tumors.[4,10] Unfortunately, several essential attributes—including timing of drug release—are difficult to control in liposome preparations, which creates substantial challenges in optimization of dose regimens. Therefore, we compared our new DOX formulations to DOXIL, to show that the more versatile PEGylated PLGA particles have the same ability to reduce toxicity and retain biological activity.

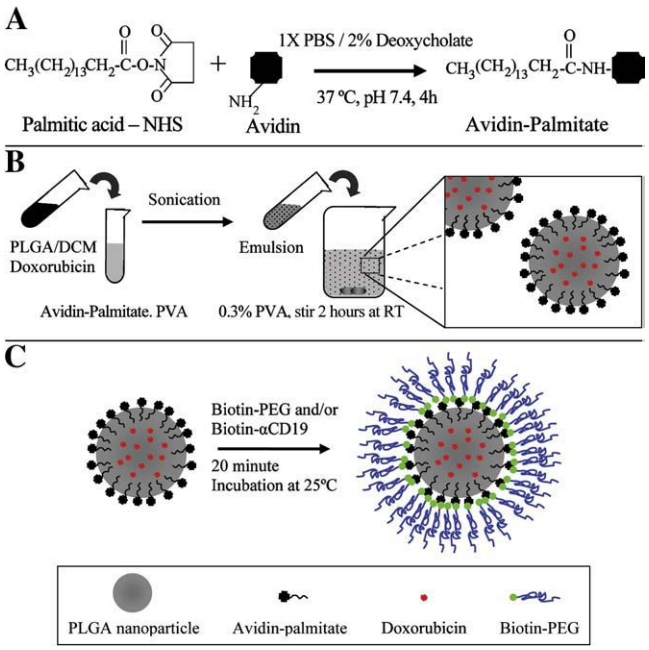

Figure 1. (**A**) Synthesis of avidin-lipid conjugate. Avidin is reacted with palmitic acid–NHS in a 2% deoxycholate buffer to form avidin-palmitate conjugate. (**B**) The conjugate is then added during the aqueous phase of a modified single-emulsion technique to form avidin-coated PLGA nanoparticles. (**C**) Avidin-coated nanoparticles can then be incubated in solution with biotinylated ligands to form surface-modified nanoparticles.

Methods

Materials

Doxorubicin hydrochloride and DOXIL were obtained from Bedford Laboratories. PLGA 50/50 with molecular weight of approximately 100,000 Da (corresponding to an inherent viscosity of 0.95–1.10 dL/g in hexafluoroisopropanol) was purchased from Absorbable Polymers, Inc. (Durect Corporation, Cupertino, California). Amine-terminated methoxypolyethylene glycol (mPEG-NH_2) with molecular weights of 5000 Da (2M2U0H01) and 10,000 Da (2M2U0L01) was purchased from Nektar Therapeutics (Birmingham, Alabama). EZ-Link Sulfo-NHS-LC-Biotin was purchased from Pierce (Rockford, Illinois), and avidin from chicken egg white (A887) was obtained from Sigma (St. Louis, Missouri). Polyvinyl alcohol (PVA, MW 30,000–70,000 Da), deoxycholate, dimethyl sulfoxide (DMSO), methylene chloride, 3-(4,5-dimethylthiazol-2-yl)-2,5-diphenyltetrazolium bromide (MTT), and all other reagents were obtained from Sigma at reagent grade or higher and used without further purification.

Animals and cell lines

Female Balb/c RW mice (8–10 weeks) were purchased from Taconic Farms (Germantown, New York). All animal protocols were approved by the Yale University Institutional Animal Care and Use Committee (IACUC). Mice were housed under standard humane conditions according to IACUC guidelines and had access to food and water ad libitum. A20 murine B-cell lymphoma cells syngeneic to the Balb/c mouse (TIB-208)[11] were obtained from American Type Culture Collection (Manassas, Virginia) and maintained in exponential growth in RPMI complete medium.

Preparation of avidin-lipid conjugate and biotin-PEG conjugates

The avidin-lipid conjugate was prepared and characterized as described[12] and is schematically represented in Figure 1. Briefly, avidin at 5 mg/mL was reacted with a 10-fold excess of NHS–palmitic acid in 1× phosphate-buffered saline (PBS) containing 2% sodium deoxycholate buffer. The mixture was sonicated in a sonic water bath briefly and gently mixed at 37°C. Reactants were dialyzed overnight against PBS containing 0.15% deoxycholate to remove excess fatty acid and hydrolyzed ester. Conjugation of the avidin-palmitate was verified by reverse-phase high-performance liquid chromatography (Shimadzu, Piscataway, New Jersey) on a Prevails C18 column (Sigma, St. Louis, Missouri) with a linear methanol gradient in PBS as the mobile phase and ultraviolet detection at 214 and 280 nm. PEG-biotin conjugates were made using sulfo-NHC-LC-biotin from Pierce. mPEG-NH_2 (MW 5 kDa or 10 kDa) was

first dissolved at 20 mg/mL in sterile 1× PBS. Sulfo-NHS-biotin was added in 20-fold molar excess and allowed to react in a glass vial with a stir bar for 4 hours at room temperature (RT) 25 ± 2°C. The resulting conjugate was dialyzed against PBS using a 3500 MW cutoff membrane. Biotin-to-PEG coupling was verified with the HABA assay (Pierce catalogue no. 28010).

Preparation of DOX-loaded, PEGylated PLGA nanoparticles

Surface-modified, DOX-loaded nanoparticles were prepared using a modified single-emulsion method (Figure 1). Ten milligrams of lyophilized doxorubicin hydrochloride were added directly to a PLGA solution of 100 mg polymer in 2 mL methylene chloride. This solution was sonicated on ice for 30 seconds at 38% amplitude (GEX600 600 W ultrasonic processor, Sigma), then added dropwise under vortex to an aqueous solution consisting of 2 mL 2.5% PVA and 2 mL avidin-palmitate conjugate solution, then sonicated for an additional 30 seconds on ice. Solvent was removed by magnetic stirring for 2 hours in 0.3% PVA at RT, and nanoparticles were collected by centrifugation at 12,000 *g* for 5 minutes and washed with sterile water to remove PVA and excess avidin-lipid. Nanoparticles were lyophilized and stored at −20°C. Biotinylated PEG was attached to nanoparticles immediately before use (Figure 1). Particles were incubated with 1000 μg of 10,000 MW PEG or 500 μg of 5000 MW (20 mg/mL in PBS) per milligram of nanoparticles and diluted with PBS to 200 μL, then incubated for 15 minutes at RT on a rotary shaker.

Nanoparticle size, loading, and controlled release

Nanoparticle size and surface morphology were characterized using scanning electron microscopy (SEM) and Scion image analysis software (Scion Corp., Frederick, Maryland). Samples for SEM were fixed on an aluminum stub using two-sided carbon tape and sputter-coated with a gold/palladium mixture (60:40) under vacuum in an argon atmosphere using a sputter current of 40 mA (Cressington 108Auto, Cressington Instruments, Watford, England, United Kingdom). The samples were imaged using a Philips XL30 Scanning Electron Microscope and LaB electron gun (FEI, Hillsboro, Oregon).

The rate of DOX release from nanoparticles was measured as a function of time during incubation in 1× PBS. Triplicate samples of 5 mg of nanoparticles were suspended in 1 mL PBS in a microcentrifuge tube and sonicated briefly in an ultrasonic water bath. The samples were then incubated on an orbital shaker at 37°C. The particles were centrifuged and supernatant removed and replaced at defined time points. The fluorescence of each supernatant sample was measured using a Molecular Devices (Sunnyvale, CA) SpectraMax M5 at excitation 470 nm/emission 590 nm to determine DOX concentration. Total nanoparticle DOX encapsulation was determined by dissolving 10 mg of sample in DMSO. Encapsulation efficiency is expressed as a percentage and was calculated by:

$$\frac{\text{Measured DOX (μg) encapsulated per mg NP}}{\text{Theoretical max loading (100 μg DOX/1 mg PLGA)}}$$

Nonspecific protein adsorption

Particles were assessed for nonspecific protein binding using Texas Red–labeled bovine serum albumin (BSA). Triplicate samples of 1 mg of unloaded "blank" nanoparticles (unmodified, avidin-coated, and PEGylated) were incubated in 1 mL PBS at 37°C, pH 7.4 with 500 μg/mL Texas Red–labeled BSA for 24 hours. Samples were centrifuged and washed three times with deionized water, then resuspended in 1 mL deionized water and dispersed through brief sonication. BSA–Texas Red content was calculated by fluorescence at excitation 590/emission 615 nm with nanoparticle (with no BSA–Texas Red incubation) background subtracted.

In vitro cytotoxicity against A20 lymphoma cells

The cytotoxic activity of DOX nanoparticles against A20 cells was compared to free drug, DOXIL, and controls using MTT to quantify cell survival. 1×10^5 A20 cells were added in 100 μL of RPMI complete medium to each well of a 96-well plate and allowed to recover for 24 hours. After recovery, free drug, blank nanoparticles, drug-loaded nanoparticles, or DOXIL were added to the wells in 100 μL medium, and control wells received 100 μL medium. DOX concentration was calculated in micromoles for 200 μL of total volume. Cells were treated for 24 hours, after which 20 μL of MTT reagent (5 mg/mL) was added to the well. After incubation for 3 hours the plates were centrifuged and the supernatant discarded. The formazan product was solubilized in 100 μL of 0.075 N acidified isopropanol (HCl) and supernatant separated from cell debris and remaining particles via centrifugation. Absorbance of the formazan solution was read at 570 nm (650 nm background) on a SpectraMax plate reader.

In vivo antitumor efficacy

In vivo efficacy of DOX-loaded nanoparticles was tested using subcutaneous A20 tumors. Twelve 8- to 10-week-old female Balb/c mice were lightly anesthetized, and 1×10^7 A20 cells in the exponential growth phase were implanted subcutaneously in a shaved portion of the left flank. Palpable tumors were established approximately 20 days after implantation, at which time animals were divided into four treatment groups with similar average starting tumor volumes: (1) no-treatment control, (2) free DOX, (3) DOXIL, and (4) DOX-loaded nanoparticles. Animals in the treatment groups received a single 6 mg/kg dose given as two 50-μL intratumoral injections on opposite sides of the tumor. Tumor growth was followed until established end points and measured using calipers and tumor volume calculated using a volumetric formula: $L \times W \times H \times {}^{\pi}/_{6}$.

DOX/nanoparticle biodistribution

Twenty-seven female Balb/c mice (8–10 weeks old) were injected with 120 μg DOX in PEGylated nanoparticles, unmodified nanoparticles, or as free drug in solution via the tail vein. At 1 hour, 1 day, and 2 days after injection, mice were killed via carbon dioxide inhalation and 0.5–1.0 mL whole blood was collected in a heparinized syringe via cardiac puncture. The blood was separated by centrifugation and plasma isolated for immediate analysis or storage at –80°C. Fifty microliters of plasma were then added to 450 mL of extraction buffer consisting of 10% Triton X-100, deionized water, and acidified isopropanol (0.75 N HCl) in a 1:2:15 volumetric ratio, and DOX was extracted overnight at –20°C. To account for drug release from the particles when generating standard curves, nanoparticles were incubated in PBS at 37°C for 1, 24, or 48 hours, then separated from the supernatant and added to aliquots of whole blood for extraction and DOX quantification. Standard curves for free drug were generated by addition of free DOX to aliquots of whole blood followed by extraction and quantification. The fluorescence of the supernatant was determined at excitation/emission of 470/590 nm to calculate DOX concentration.

Evaluation of DOX-induced cardiomyopathy

Cardiotoxicity was assessed using echocardiography, serum creatine phosphokinase (CPK) levels, and histological examination. These studies were performed in 14 female Balb/c mice (8–10 weeks old) weighing approximately 20 g. Mice received intravenous injections of saline, free DOX, DOXIL, or PEGylated DOX-loaded nanoparticles via the tail vein. Mice in the treatment groups received three injections of 6 mg/kg DOX per dose (in 200 μL saline) for a total cumulative dose of 18 mg/kg, a dose known to result in DOX-induced cardiomyopathy in mice.[13] Mice in the control group received 200 μL of saline each time.

Two weeks after the final dose, mice were lightly anesthetized with 1% isoflurane, had their chest hair removed with a depilatory, and were imaged via echocardiography. M-mode images of the left ventricle (LV) were acquired using a 15-MHz probe and Sonos 7500 ultrasound system (Philips Healthcare, Andover, Massachusetts) in the long and short axes to acquire end-systolic and end-diastolic measurements of anterior and posterior wall thicknesses and cavity diameter. Cardiac function was assessed by calculating fractional shortening, defined as ($LV_{\text{end diastolic}}$ diameter − $LV_{\text{end systolic}}$ diameter)/($LV_{\text{end diastolic}}$ diameter).

Mice were killed after echocardiography, blood was collected in heparinized tubes via cardiac puncture, and the hearts were removed and perfused with PBS containing 0.16 mg/mL heparin. Cardiac tissue was homogenized in ice-cold PBS (10 mL/g tissue) and centrifuged at 1500 *g* for 5 minutes (for superoxide dismutase assay) or at 10,000 *g* for 10 minutes (for reduced glutathione and glutathione peroxidase assay) at 4°C. Superoxide dismutase and glutathione peroxidase enzymatic activity and total reduced glutathione were measured using kits from Cayman Chemical (Ann Arbor, Michigan). The blood serum was analyzed for CPK activity. Small samples of the LV were held for histological examination. Tissue was formalin-fixed, dehydrated, and stained with hematoxylin and eosin and with Masson's trichrome for analysis under light microscopy. Samples were examined by an experienced pathologist for DOX-induced histopathological changes.

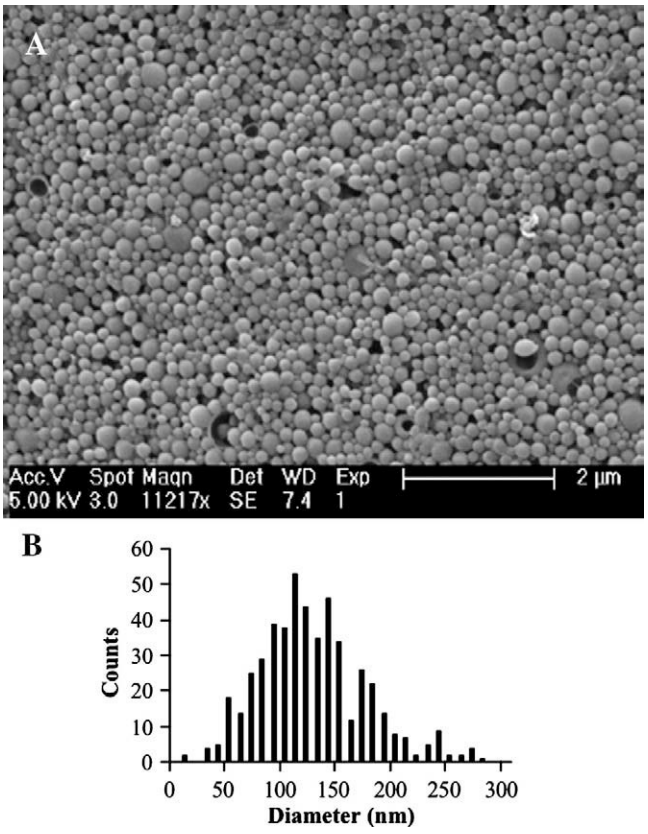

Figure 2. (**A**) SEM image of DOX-loaded PLGA nanoparticles. Samples were imaged on a Philips XL30 system at 10 kV. (**B**) Representative size distribution of nanoparticles compiled using SEM data analyzed by Scion image processing software. The mean size was found to be 126 nm with a standard deviation of 50 nm, and the maximum and minimum observed diameters were 280 and 30 nm, respectively (n = 500).

Results

Particle characterization

PLGA nanoparticles were found to have an average diameter of 130 nm with a smooth and spherical surface morphology (Figure 2). High loading of DOX, up to nearly 5% drug wt/wt (47 μg DOX per mg nanoparticles), was achieved and released in a sustained fashion into PBS (Figure 3). Encapsulation efficiency was found to be 47%. The in vitro release was biphasic (Figure 3): approximately 50% of encapsulated DOX was released from nanoparticles during

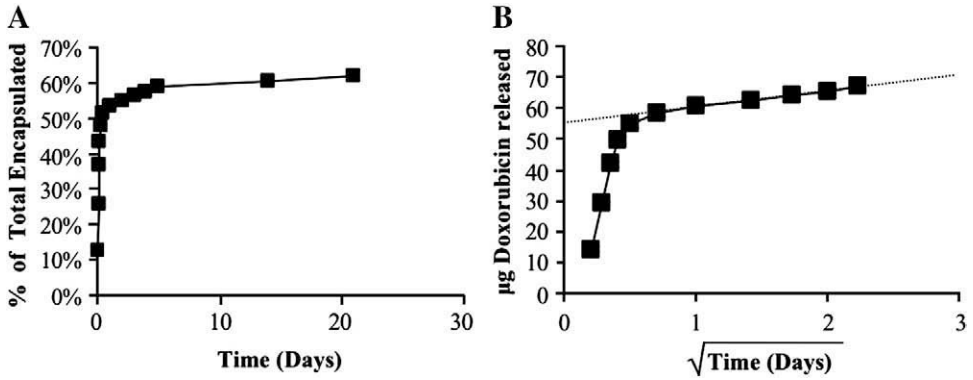

Figure 3. Cumulative release of DOX from PLGA nanoparticles. Triplicate samples of 5 mg nanoparticles were incubated in 1 mL of PBS at 37°C in a rotary shaker. DOX fluorescence was read at excitation/emission 470/590 nm to determine DOX concentration. (**A**) The cumulative amount of DOX release per milligram of nanoparticles is shown as a percentage of the total DOX encapsulated. (**B**) The total mass of DOX (μg) released per milligram of nanoparticles is shown as a function of the square root of time, demonstrating a biphasic release curve with an initial burst preceding diffusion-mediated release. Error bars not visible are smaller than data markers ($n = 3$).

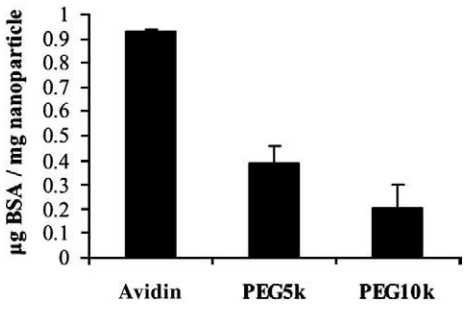

Figure 4. Nonspecific protein adsorption on PEGylated nanoparticles. Blank nanoparticles (avidin-coated, or PEG-coated) were incubated in triplicate for 24 hours under physiologic conditions with Texas Red–labeled BSA. Samples were then washed three times to remove excess BSA, and surface-bound protein was measured spectrofluorimetrically. The data are normalized to values for blank nanoparticles incubated in 1× PBS without BSA–Texas Red. The differences between each group are statistically significant ($P < .05$).

the first 24 hours of incubation. After this initial burst release, DOX was released continuously at a linear rate with respect to the square root of time, reflecting diffusion-mediated release from the nanoparticles. Nanoparticles were later removed from the saline and dissolved in DMSO to determine residual loading. Using this method it was possible to account for greater than 90% of total encapsulated DOX.

In vitro characterization of nanoparticle surface

The amount of surface-bound avidin was determined directly by micro-bicinchoninic acid (BSA) assay: DOX-loaded nanoparticles were found to incorporate 35 ± 5 μg avidin per milligram of nanoparticles. To estimate the potential interaction of serum proteins with nanoparticles, avidin-modified particles were surface-modified with different molecular-weight lengths of biotinylated PEG and subsequently incubated with Texas Red–labeled BSA under physiological conditions for 24 hours. BSA was found to adsorb to avidin-coated particles but to a much lower extent on PEGylated particles (Figure 4). The incorporation of avidin molecules on the nanoparticle surface resulted in the adsorption of nearly 1 μg BSA per milligram of avidin-coated nanoparticles. Pretreatment of avidin-coated particles with 5000 MW biotin-PEG reduced protein adsorption to less than 0.5 μg BSA per milligram of nanoparticles; pretreatment with the same molar quantity of 10,000 MW PEG reduced adsorption to less than 0.25 μg BSA per milligram of nanoparticles.

Nanoparticle cytotoxicity

The biological activity of PEGylated DOX-loaded nanoparticles against A20 murine lymphoma cells was quantified using the MTT cytotoxicity assay. Cytotoxicity of PEGylated nanoparticles was compared to free DOX, DOXIL, non-drug-loaded nanoparticles, and no treatment. Drug-loaded nanoparticles were found to be more toxic to A20 cells than free drug: extrapolation from the dose-response curve demonstrates that a dose of 1 μM free DOX killed 40% of the cell population after 24 hours, whereas a dose of 1 μM DOX in nanoparticles killed nearly 60% of the population (Figure 5, *A*). Blank particles, with or without surface modification, did not influence the growth or viability of cells in culture; doses of blank nanoparticles up to 10 mg/mL did not influence cell growth. Treatment with free DOX was not found to be more potent when administered simultaneously with blank particles (Figure 5, *B*).

Nanoparticle efficacy

PEGylated nanoparticles were shown to have efficacy against a solid tumor developed using A20 cells. Subcutaneous administration of 1×10^7 A20 cells in the left flank of 8- to 10-week-old Balb/c mice resulted in palpable spherical tumors at approximately 20 days. Animals were treated with a single

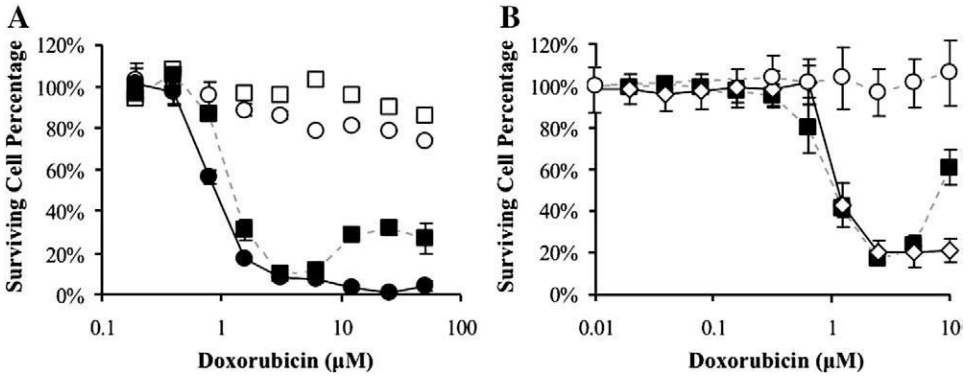

Figure 5. (**A**) Cytotoxicity of DOX in PEGylated nanoparticles (●), DOXIL (□), or free DOX (■) versus no treatment (○) against A20 lymphoma cells after 24 hours of treatment. Cell survival was assessed via MTT assay and comparison to a standard curve established with known numbers of cells. (**B**) Cytotoxicity of free DOX (■) as compared to free DOX co-administered with blank unloaded nanoparticles (◊) and blank unloaded nanoparticles alone (○). Error bars not visible are smaller than data markers ($n = 3$). The difference in half-maximal inhibitory concentration (IC_{50}) for free drug versus PLGA nanoparticle groups was not statistically significant.

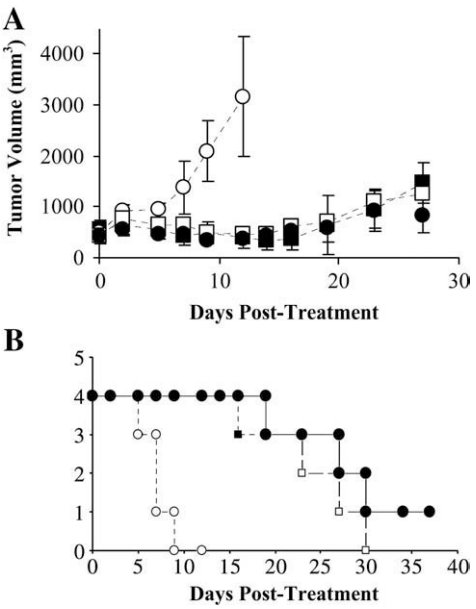

Figure 6. (**A**) Intratumoral treatment of subcutaneous A20 tumor. Female Balb/c mice (8–10 weeks old) were given 1×10^7 A20 cells subcutaneously in the left flank, resulting in palpable solid tumors 20 days after implantation. At that time animals received a single intratumoral dose of: (1) saline (○), (2) free DOX (■), (3) DOXIL (□), or (4) DOX-loaded nanoparticles (●) ($n = 4$ per treatment group). (**B**) Survival curve for treated mice. Differences in tumor growth and survival times between treatment groups were not statistically significant.

intratumoral dose of either saline (no treatment control), or 6 mg/kg of free DOX, DOXIL, or DOX-loaded nanoparticles. DOX-loaded nanoparticles were found to be as effective as free drug and DOXIL in suppressing tumor growth (Figure 6).

Doxorubicin serum clearance and biodistribution

DOX concentration in the serum was measured after administration of a single intravenous dose of either modified (PEGylated) or unmodified (avidin-coated) DOX-loaded nanoparticles. PEGylation of the PLGA nanoparticles was found to significantly increase the retention time of DOX in the blood. DOX was not detected in the serum of animals receiving either free DOX or avidin-coated (unmodified) DOX-loaded nanoparticles 24 hours after administration. In contrast, approximately 40% of the initial dose (6 μg) was still present in the serum 24 hours after intravenous injection of PEGylated DOX nanoparticles (Figure 7, *A*). DOX fluorescence was not observed in the serum of animals injected with blank nanoparticles. Additionally, six separate mice were given a single dose of 2 μg DOX either as free drug or in PEGylated nanoparticles. One hour after administration, the vast majority of free DOX was extracted from the liver and kidneys, whereas approximately 30% of the initial dose of DOX distributed to the serum when given via PEGylated nanoparticles (Figure 7, *B*).

In vivo cardiotoxicity

To assess the cardiotoxicity of various forms of intravenous DOX, mice were administered either saline or DOX delivery systems containing a total cumulative dose of 18 mg/kg DOX, a dose known to cause cardiomyopathy detectable by enzymatic, functional, and histopathological changes in mice receiving free DOX. Analysis was conducted 2 weeks after the final treatment to distinguish persistent cardiotoxic effects from acute (<72 hours) changes. At the time of analysis there were no statistically significant differences in overall or cardiac tissue mass between any of the groups.

Serum CPK levels are a well-characterized marker for cellular damage in a variety of cardiac disease models. The greatest magnitude of CPK change was observed in the serum of DOX-treated mice, with more than a sevenfold increase in enzyme level as compared with untreated mice

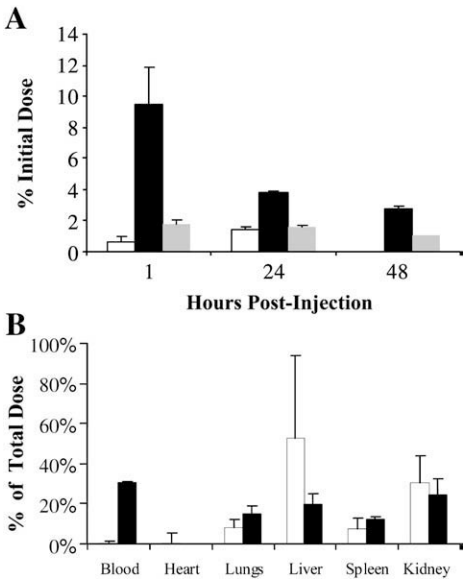

Figure 7. (**A**) Serum levels of DOX following injection of PEGylated (*black bars*), avidin-coated unPEGylated (*grey bars*) DOX-loaded nanoparticles, or free DOX (*white bars*) in female Balb/c mice (8–10 weeks old). Animals received 6 μg DOX, or nanoparticle equivalent, via intravenous tail vein injection. At various time points mice were killed (n = 3 per treatment group, per time point; 27 mice total) and blood collected via cardiac puncture for spectrofluorimetric determination of DOX concentration. (**B**) Representative biodistribution of PEGylated, DOX-loaded nanoparticles (*black bars*) compared to free drug (*white bars*) at 1 hour after intravenous injection. Three mice per treatment group (six mice total) were given a total dose of 2 μg DOX via the tail vein and killed 1 hour after injection. The major organs were excised and homogenized; DOX was extracted using acidified isopropanol and quantified spectrofluorimetrically.

(Table 1). Levels of cardiac glutathione peroxidase were also increased in animals receiving free DOX. The activity of superoxide dismutase was not statistically different; catalase activity was not examined because of its low levels in the heart as well as previous evidence indicating that DOX does not induce changes in cardiac catalase levels or activity.[14] DOX in nanoparticles showed the smallest change in glutathione peroxidase and CPK of all the DOX-treated groups.

The two most common methods for monitoring anthracycline-induced cardiac changes are echocardiography and histology. Measurement of LV ejection fraction or fractional shortening can be used to follow DOX-induced cardiac damage in small animals.[15,16] In this study animals treated with free DOX showed a statistically significant, absolute decrease of 12% in LV fractional shortening compared with control animals (Table 1). This decrease is consistent with DOX-induced damage and impaired cardiac function. No changes in fractional shortening were observed in animals treated with PEGylated DOX nanoparticles or DOXIL (Table 1). There were no significant histopathological alterations in any of the treatment groups, although this finding is more likely due to the time frame of the study rather than consequences, or lack thereof, of DOX treatment.

Table 1
DOX-induced changes in left ventricular function and GSHPx and serum CPK activities at 2 weeks after last injection *

Treatment group	GSHPx (nmol/min/mg protein)	LV fractional shortening (%)	Serum CPK (U/mL)
Saline	170 ± 8	54 ± 2	96 ± 0
DOX	232 ± 3 †	42 ± 5 †	697 ± 136 †
DOXIL	117 ± 15 †	57 ± 2	360 ± 27 †
Nanoparticle (PEG)	177 ± 5	56 ± 2	164 ± 96

CPK, creatine phosphokinase; GSHPx, glutathione peroxidase.
*Ventricular function was measured by echocardiography and calculation of fractional shortening. Data are the mean ± SD for three to four mice. Heart tissue was then perfused with PBS buffer containing 0.16 mg/mL heparin, homogenized in ice-cold PBS, and analyzed using kits from Cayman Chemical. Data are mean ± SD for three to four mice. Free DOX administration significantly increased serum CPK levels ($P < .05$) and decreased LV fractional shortening ($P < .05$).
†Differs significantly from control/saline value ($P < .05$).

Discussion

PEGylation has long been recognized as a useful tool for increasing the circulation of drug delivery carriers; discovery of a reliable method of PEGylating liposomes transformed the use of DOX and other drugs such as cytokines and monoclonal antibody Fab fragments[17] and demonstrated the clinical viability of liposomal drug delivery systems. The development of PEGylated polymeric nanoparticles, however, has lagged behind that of liposomes largely because of the difficulties associated with creating functionalized particle surfaces. In this investigation, biotinylated PEG was used to surface-modify DOX-loaded, avidin-coated nanoparticles for the purposes of reticuloendothelial system and cardiac avoidance. Our results show that the benefits of this approach include both improved safety (decreased cardiotoxicity) as well as increased efficacy (cytotoxicity against lymphoma cells) of the encapsulated DOX.

The pharmacokinetics of intravenous administration of DOX in mice and humans are well documented. Free DOX undergoes two separate phases of clearance, the first being an extremely rapid distribution out of the blood and into tissues, with a half-life of the order of 5 minutes across most species; one study that followed DOX plasma concentrations after a single 250-μg intravenous dose in nude mice detected less than 1 μg/mL plasma 5 minutes post-injection.[18] In this study it was found that circulation of PLGA nanoparticles loaded with DOX could be improved by PEGylation; approximately 3% of the initial dose of nanoparticles was still detected in the serum 48 hours after initial administration. As a result of the rapid clearance of free DOX, drug found in the serum is believed to be encapsulated in nanoparticles. Unmodified/non-PEGylated DOX nanoparticles improved delivery over that of free DOX but were found

to be cleared more rapidly than comparable, PEGylated particles, with a fivefold lower dose being detected in the serum 1 hour after injection, and twofold lower doses detected 24 and 48 hours after injection. Whereas the avidin groups on the PEGylated particles are bound by biotinylated PEG so that the entire particle is effectively shielded by a steric PEG barrier, the avidin on unmodified particles probably promotes protein binding (Figure 4), particle opsonization, and clearance.

Importantly, encapsulation of DOX in PEGylated nanoparticles was found to decrease cardiotoxicity compared with free drug. Injection into mice of a dose producing measurable toxicity (18 mg/kg)—as measured by enzymatic and functional tests—in animals receiving free drug did not produce measurable toxicity in either the liposomal or nanoparticle formulation. Using echocardiography, one of the most clinically relevant and predictive measures of DOX-induced cardiotoxicity, it was found that DOX-treated mice experienced a statistically significant absolute drop of over 10% in LV fractional shortening (compared with the control group), indicating the onset of cardiac damage. The average fractional shortening value of 40% in the DOX group is near the absolute lowest threshold of acceptable normal values for healthy animals.[15] There was also a 600% increase in the serum CPK values for animals in the DOX treatment group. The slight increase observed in DOXIL-treated animals is probably due to skeletal (as opposed to cardiac) CPK release, which is confirmed by the lack of elevated reduced glutathione levels in these animals. Although there were no significant findings histologically, our analysis was done only 2 weeks after completion of treatment. Therefore, it is likely that not enough time had elapsed to discern major histological changes.

Cardiotoxicity was significantly reduced by encapsulation in nanoparticles, whereas antitumor activity was preserved against A20 lymphoma cells in vitro (Figure 5). The dose-response curve of free drug matched expected values. We note that the decrease in cytotoxicity observed at high DOX concentrations of free DOX (>10 μM) may be due to formation of aggregates (i.e., DOX micelles) and subsequent decrease in transport and activity[19] and not to any problem with the formulation or assay itself. DOXIL was not found to have any effect at clinical concentrations. This was expected, because DOXIL is stable in saline or cell culture even under physiological conditions; release of DOX from DOXIL is mediated at the tissue level through processes that are still not fully understood. This, in fact, remains a major problem with DOXIL as a delivery system for DOX.[20] Blank avidin-coated and unmodified nanoparticles were not found to have any stimulatory or cytotoxic effect by themselves; although blank nanoparticles demonstrate a cytotoxic effect at 10 mg/mL (data not shown), this translates to a very large dose of particles unlikely to be used in any in vivo situation.

We note that encapsulation of DOX within PLGA nanoparticles seemed to enhance cytotoxicity of the drug: the IC_{50} for free DOX was approximated to be 2.6 μM, whereas the IC_{50} for PEGylated nanoparticle DOX was 1.8 μM. This finding was surprising as the in vitro release kinetics (Figure 3) indicate that a majority greater than 50% of encapsulated DOX is still retained in the nanoparticles—and therefore unavailable to exert a cytotoxic effect—by the conclusion of the 24-hour treatment period. Moreover, co-administration of blank nanoparticles with free drug did not alter the dose-response curve (Figure 5*B*), suggesting that there is no synergistic cytotoxic effect between non-drug-loaded nanoparticles and free DOX. Therefore, we conclude that the observed cytotoxic effect of DOX-loaded PLGA nanoparticles cannot solely be dependent upon free drug released into the surrounding medium from degrading nanoparticles but must depend on uptake of nanoparticles by cells and enhanced effectiveness of DOX released intracellularly.

The cytotoxic effect may be a product of the mechanism of release of DOX from the particles. In related work we have found that PLGA nanoparticles can be internalized by phagocytic processes followed by endosomal escape and delivery of encapsulated agents to the cytosol.[21] Improved intracellular delivery would greatly improve the efficacy of DOX, and smaller doses delivered via this mechanism would be capable of exerting cytotoxic effects comparable to those obtained with higher extracellular concentrations of free drug. The exact mechanism remains unclear at this time, and further experiments are planned to observe the intracellular delivery and release of DOX. One interesting finding from these experiments may be the effect of high intracellular doses of DOX delivered by nanoparticles on previously anthracycline-resistant and multidrug-resistant tumor cells, consistent with previous studies demonstrating that DOX-loaded nanoparticles may overcome tumor cell multidrug resistance.[22-24]

PLGA nanoparticles have advantages over other drug delivery vehicles. This polymer is US Food and Drug Administration–approved for a variety of applications and has been in use in humans for over 30 years; the amount and rate of drug release can be controlled via mechanisms that are well known; and a wide array of molecules—large and small, hydrophobic and hydrophilic—can be encapsulated within PLGA. In this report a new surface coupling system[12] was demonstrated to be robust and effective. The clinical potential of this system was confirmed by improved circulation, by preserved bioactivity, and by the cardioprotective effects of the PEGylated particles. If the lipid-mediated coupling system used in these studies were unstable, then it would be difficult to explain the extended blood circulation time and cardioprotective effects seen with the PEGylated particles. This surface modification technique has broader significance in that it allows for the rapid, facile evaluation of multiple surface ligands and the effect of ligand density for targeted nanoparticle applications. Due to the use of avidin at the particle surface, a multitude of biotinylated ligands or even combinations of

ligands can be attached in precise fashion after particle manufacture. The versatility of this method, however, is the ability to easily assess other surface modifications, such as the attachment of biotinylated antibodies, aptamers, or proteins for active targeting purposes, allowing for the site-specific delivery of drug-loaded PLGA nanoparticles to targeted cells and tissues.

References

1. Soppimath KS, Aminabhavi TM, Kulkarni AR, Rudzinski WE. Biodegradable polymeric nanoparticles as drug delivery devices. J Control Release 2001;70:1-20.
2. Anderson JM, Shive MS. Biodegradation and biocompatibility of PLA and PLGA microspheres. Adv Drug Deliv Rev 1997;28:5-24.
3. Okada H, Toguchi H. Biodegradable microspheres in drug-delivery. Crit Rev Ther Drug Carrier Syst 1995;12:1-99.
4. Goren D, Horowitz AT, Tzemach D, Tarshish M, Zalipsky S, Gabizon A. Nuclear delivery of doxorubicin via folate-targeted liposomes with bypass of multidrug-resistance efflux pump. Clin Cancer Res 2000;6: 1949-57.
5. Moghimi SM, Szebeni J. Stealth liposomes and long circulating nanoparticles: critical issues in pharmacokinetics, opsonization and protein-binding properties. Prog Lipid Res 2003;42:463-78.
6. Faraasen S, Voros J, Csucs G, Textor M, Merkle HP, Walter E. Ligand-specific targeting of microspheres to phagocytes by surface modification with poly(L-lysine)-grafted poly(ethylene glycol) conjugate. Pharm Res 2003;20:237-46.
7. Gref R, Luck M, Quellec P, Marchand M, Dellacherie E, Harnisch S, et al. 'Stealth' corona-core nanoparticles surface modified by polyethylene glycol (PEG): influences of the corona (PEG chain length and surface density) and of the core composition on phagocytic uptake and plasma protein adsorption. Colloids Surfaces B–Biointerfaces 2000;18:301-13.
8. Li YP, Pei YY, Zhang XY, Gu ZH, Zhou ZH, Yuan WF, et al. PEGylated PLGA nanoparticles as protein carriers: synthesis, preparation and biodistribution in rats. J Control Release 2001;71:203-11.
9. Yeh ET, Tong AT, Lenihan DJ, Yusuf SW, Swafford J, Champion C, et al. Cardiovascular complications of cancer therapy: diagnosis, pathogenesis, and management. Circulation 2004;109:3122-31.
10. Allen TM, Martin FJ. Advantages of liposomal delivery systems for anthracyclines. Semin Oncol 2004;31:5-15.
11. Biragyn A, Kwak LW. Models for lymphoma. In: Coico R, editor. Current protocols in immunology. Hoboken, NJ: John Wiley and Sons, Inc.; 2001. p. 20.6.1-20.6.30.
12. Fahmy TM, Samstein RM, Harness CC, Saltzman WM. Surface modification of biodegradable polyesters with fatty acid conjugates for improved drug targeting. Biomaterials 2005;26:5727-36.
13. Myers CE, McGuire WP, Liss RH, Ifrim I, Grotzinger K, Young RC. Adriamycin: the role of lipid peroxidation in cardiac toxicity and tumor response. Science 1977;197:165-7.
14. Kang YJ, Chen Y, Epstein PN. Suppression of cardiotoxicity by overexpression of catalase in the heart of transgenic mice. J Biol Chem 1996;271:12610-6.
15. Teraoka K, Hirano M, Yamaguchi K, Yamashina A. Progressive cardiac dysfunction in adriamycin-induced cardiomyopathy rats. Eur J Heart Fail 2000;2:373-8.
16. Jacoby JJ, Kalinowski A, Liu MG, Zhang SSM, Gao Q, Chai GX, et al. Cardiomyocyte-restricted knockout of STAT3 results in higher sensitivity to inflammation, cardiac fibrosis, and heart failure with advanced age. Proc Natl Acad Sci U S A 2003;100:12929-34.
17. Davis ME, Chen Z, Shin DM. Nanoparticle therapeutics: an emerging treatment modality for cancer. Nat Rev Drug Discov 2008;7:771-82.
18. Johansen PB. Doxorubicin pharmacokinetics after intravenous and intraperitoneal administration in the nude-mouse. Cancer Chemother Pharmacol 1981;5:267-70.
19. Bouma J, Beijnen JH, Bult A, Underberg WJM. Anthracycline antitumour agents. Pharm World Sci 1986;8:109-33.
20. Allen TM, Mumbengegwi DR, Charrois GJR. Anti-CD19-targeted liposomal doxorubicin improves the therapeutic efficacy in murine B-cell lymphoma and ameliorates the toxicity of liposomes with varying drug release rates. Clin Cancer Res 2005;11:3567-73.
21. Shen H, Ackerman AL, Cody V, Giodini A, Hinson ER, Cresswell P, et al. Enhanced and prolonged cross-presentation following endosomal escape of exogenous antigens encapsulated in biodegradable nanoparticles. Immunology 2006;117:78-88.
22. Lamprecht A, Benoit JP. Etoposide nanocarriers suppress glioma cell growth by intracellular drug delivery and simultaneous P-glyco-protein inhibition. J Control Release 2006;112:208-13.
23. Soma CE, Dubernet C, Barratt G, Nemati F, Appol M, Benita S, Couvreur P. Ability of doxorubicin-loaded nanoparticles to overcome multidrug resistance of tumor cells after their capture by macrophages. Pharm Res 1999;16:1710-6.
24. Wong HL, Bendayan R, Rauth AM, Wu XY. Simultaneous delivery of doxorubicin and GG918 (Elacridar) by new Polymer-Lipid Hybrid Nanoparticles (PLN) for enhanced treatment of multidrug-resistant breast cancer. J Control Release 2006;116:275-84.